

Jan ZWOLAK*, Marek MARTYNA**, Dominik KOZIK***

DISTRIBUTION OF CONTACT STRESSES AND INTER-TOOTH SLIP IN BILATERAL AND UNILATERAL ENGAGEMENT

ROZKŁAD NAPRĘŻEŃ KONTAKTOWYCH I POŚLIZGU MIĘDZYZĘBNEGO W ZAZĘBIENIU DWUSTRONNYM I JEDNOSTRONNYM

Key words:

toothed transmission, correction factor, unilateral and bilateral engagement.

Abstract:

The paper presents the issues concerning contact stresses and inter-tooth slip of a power shift gear used in the powertrain of a wheel loader. The kinematic diagrams on individual gear ratios of the transmission are presented. Using appropriate numerical values of contour shift coefficients (correction coefficients), normal bilateral gearing, pre-pitch unilateral gearing, and post-pitch unilateral gearing were considered. In each of the three types of gearing, contact stresses and inter-tooth slip were calculated for each gear pair and at each gear ratio level, using an author's computer program with multi-criteria optimization.

Słowa kluczowe:

przekładnia zębata, współczynnik przesunięcia zarysu, zazębienie dwustronne i jednostronne.

Streszczenie:

W pracy przedstawiono zagadnienia dotyczące naprężeń kontaktowych i poślizgu międzyzębne przekładni zębatej power shift stosowanej w układzie napędowym ładowarki kołowej. Na przedmiotowej przekładni zaprezentowano schematy kinematyczne na poszczególnych stopniach przełożenia. Stosując odpowiednie wartości liczbowe współczynników przesunięcia zarysu (współczynników korekcji) rozważano zazębienie dwustronne normalne, zazębienie jednostronne przedbiegunowe oraz zazębienie jednostronne pozabiegunowe. W każdym z trzech rodzajów zazębienia dokonano obliczeń naprężeń kontaktowych oraz poślizgów międzyzębnych dla każdej pary zębatej i na każdym stopniu przełożenia, stosując autorski program komputerowy z optymalizacją wielokryterialną.

INTRODUCTION

In the design and fabrication of gears assembled into the appropriate gear pairs to create more or less complex gear trains, the addendum modification coefficients (correction factors) are used in a fairly wide range. The numerical values of these coefficients have an impact on the characteristics of engagement, which may be defined as normal bilateral engagement, unilateral pre-pitch point engagement, and unilateral post-pitch point engagement.

The normal bilateral engagement is generated by two gears, whose respective correction factors satisfy the equation: $x_1 < 1$ for the driving gear and $x_2 > -1$ for

the driven gear. The correction factors, thus defined, cause the total length of the line of action to extend on either side of the pitch point, that is, on the side of the driving gear and the driven gear. In this case, the inter-tooth slip vectors' senses at the working depth of the gear are pointing from the pitch point towards the top land and the dedendum. Meanwhile, in the driven gear, the slip vectors' senses are pointing from the top land and dedendum towards the pitch point. Slippage directions along the outline of the working surface of the driving gear and the driven gear that are aligned with the movement direction of their contacting surface are termed positive; whereas, the slippage directions opposite to the movement direction of the contacting

* ORCID: 0000-0002-9231-6306. The Jan Grodek State University in Sanok, Mickiewicza 21 Street, 38-500 Sanok, e-mail: jazwol@ur.edu.pl.

** ORCID: 0000-0003-0622-8375. Liugong Dressta Machinery Sp. z o.o., Kwiatkowskiego 1 Street, 37-450 Stalowa Wola, e-mail: marek.martyna@dressta.com.

*** ORCID: 0000-0001-8134-3408. Center of New Technologies Dominik Kozik in Rzeszów, Szwoleżerów 2 Street, 35-216 Rzeszów e-mail: mechatron1@wp.pl.

tooth surfaces are termed negative. In order to facilitate the determination of the slip vector sense, it was established to state that on the faces of the cooperating teeth occur the positive slippages, whereas on the flanks occur the negative.

On the lateral surfaces of the teeth of the cooperating gears, there is also a friction force, whose vector changes its sense as well in relation to the pitch point. The constant change of the senses of friction forces under high cyclic loading causes an accelerated wear of the tooth top layer within the working depth. The results of our original studies, as well as of other authors, point out a pitting-induced cumulative damage build-up in the top layer on the dedendum, particularly in the area of unilateral engagement.

In the unilateral pre-pitch point engagement, as well as in the post-pitch point one, the line of action extends on one side of the pitch point and the sense of the inter-tooth slip vector does not change there. In the unilateral post-pitch point engagement, the slip vectors are oriented from the top land towards the dedendum both in the case of driving and driven gear. On the other hand, in unilateral post-pitch point engagement inter-tooth slippages in the driving and driven gear are directed from the dedendum towards the top land.

POWER SHIFT GEAR TRAIN AS A TEST OBJECT

A large number of numerical tests were conducted on the actual power shift gear train [L. 1, 2, 3, 5, 8] with a transmission ratio of 6 degrees, used in the wheel

loader propulsion system. The kinematic diagram of the gear train in the axial system is shown in Fig. 1.

The typical feature of the power shift gear train is that all gears are continuously engage with each other and the transmission is enabled under full load by means of the clutches integrated with the gears and corresponding shafts. The gear z_1 is integrated with the clutch S_p and the input shaft I, while the gear z_2 with clutch S_w and also with Shaft I. Using the clutch S_p and S_w enables a vehicle to move forwards and backwards, respectively, and these two clutches are termed directional clutches. The other clutches, such as S_1 integrated with the gear z_6 , S_2 with the gear z_8 , and S_3 with the gear z_{10} , are counted among the group of gear clutches. Gears z_3 , z_4 , z_5 , z_7 , z_9 , z_{11} , and z_{12} are connected with the respective shafts by means of a spline in such a way that no axial shifting is possible. Configuration of gears, shafts, and clutches shown in Fig. 1 allows for realization of six transmission ratios (6 forwards and 3 backwards). A complete gear train is composed of 12 gears that form 7 gear pairs while engagement. The respective gear pairs connected with each other through shafts and clutches, starting at the driving gears z_1 and z_2 , remain in the kinematic chain on the transmission ratios from 1 to 6, causing vehicle to move forwards and backwards. The gear pairs in the kinematic chain of the ratios from 1 to 6 are shown in Figs. 2 to 3.

In the gear pairs shown in Figs 2 and 3, which form kinematic chains on the sequential transmission ratios, it is observed that most gears (namely 8) take part in realization of the 4th transmission ratio. It is also observed that a gear in a given operation period is subjected to the biggest number of cycling loadings, because it is

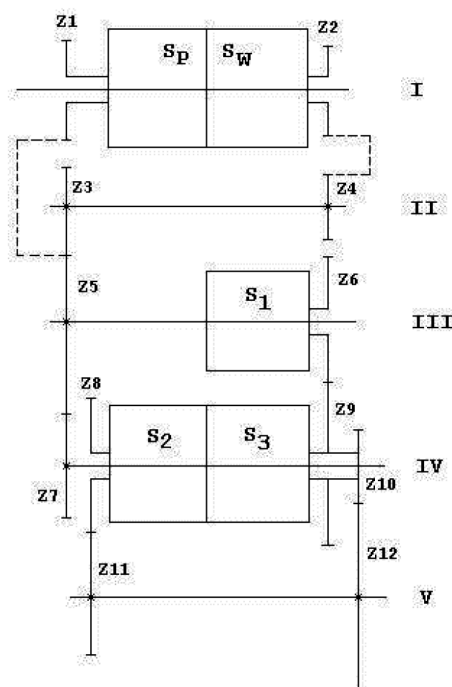


Fig. 1. Kinematic diagram of the gearbox axial alignment
Rys. 1. Schemat kinematyczny przekładni w układzie osiowym

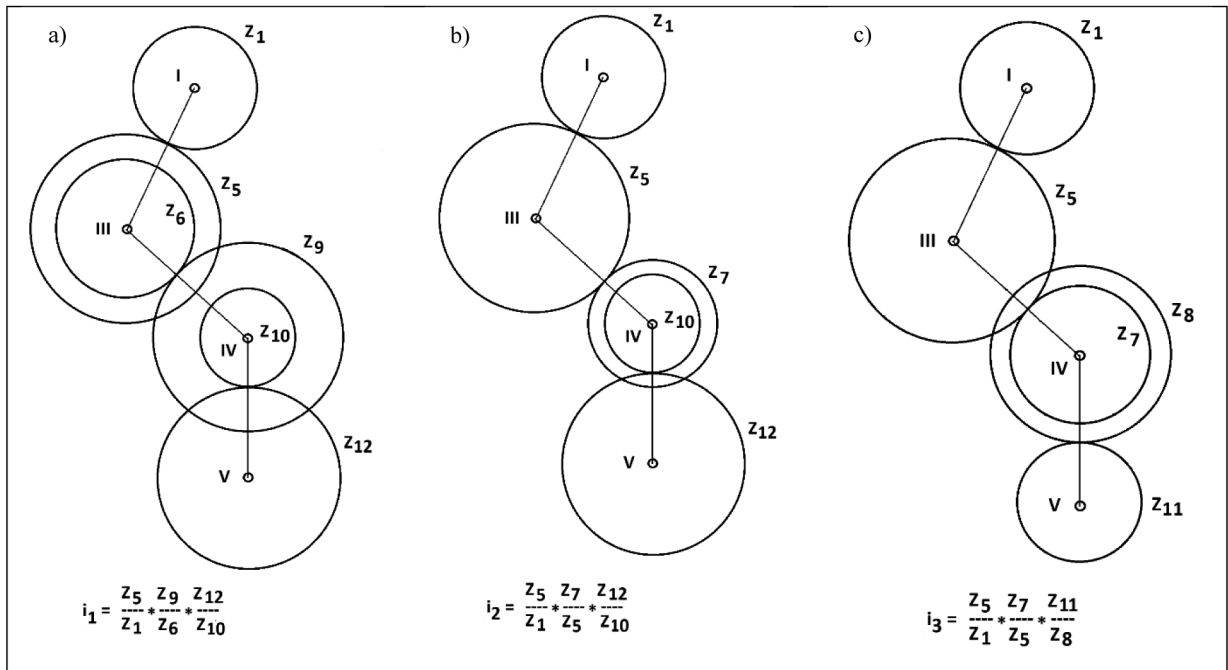


Fig. 2. Gears in realization of the transmission: a) 1 ratio, b) 2 ratio, c) 3 ratio
 Rys. 2. Koła zębate w realizacji przełożenia: a) 1 stopnia, b) 2 stopnia, c) 3 stopnia

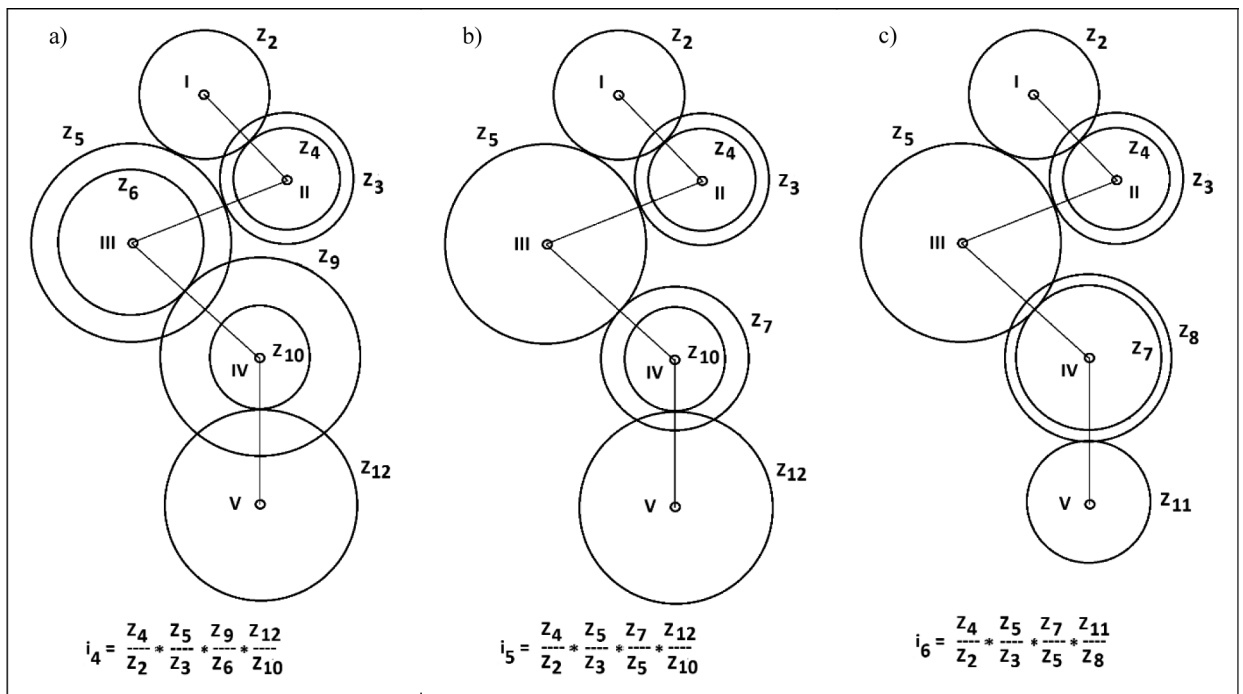


Fig. 3. Gears in realization of the transmission: a) 4 ratio, b) 5 ratio, c) 6 ratio
 Rys. 3. Koła zębate w realizacji przełożenia: a) 4 stopnia, b) 5 stopnia, c) 6 stopnia

engage with the gears z_1 , z_3 , and z_7 . Accordingly, there is a probable danger of damaging the working surface of this gear through pitting in the first instance. Among the clutches with the longest lifespan is the clutch S_3 , executing the transmission on stages 1 and 2, as well as

on 4 and 5. Meanwhile, the smallest share (only at the 3rd and 6th transmission ratio) in the load transfer refers to the clutch S_2 , which is integrated with the gear z_8 and forms a gear pair with the gear z_{11} connected by means of a spline with the output shaft V.

NORMAL BILATERAL ENGAGEMENT

In general, any gear pair consisting of gears z_1 and z_2 is in the normal bilateral engagement when [L. 4, 6] the addendum modification coefficients meet the equations: $x_1 < 1$ and $x_2 > -1$. The analysis will be carried out on

the gear pair $z_1:z_5$ of the gear train from Fig. 1, where the gear z_1 is a driving gear and z_2 a driven one. Limitations of the addendum modification coefficients, given this way, cause the total length of the action line E_1E_5 to be located on both sides of the pitch Point C. A model of engagement and the inter-tooth forces acting between the teeth are shown in Fig. 4.

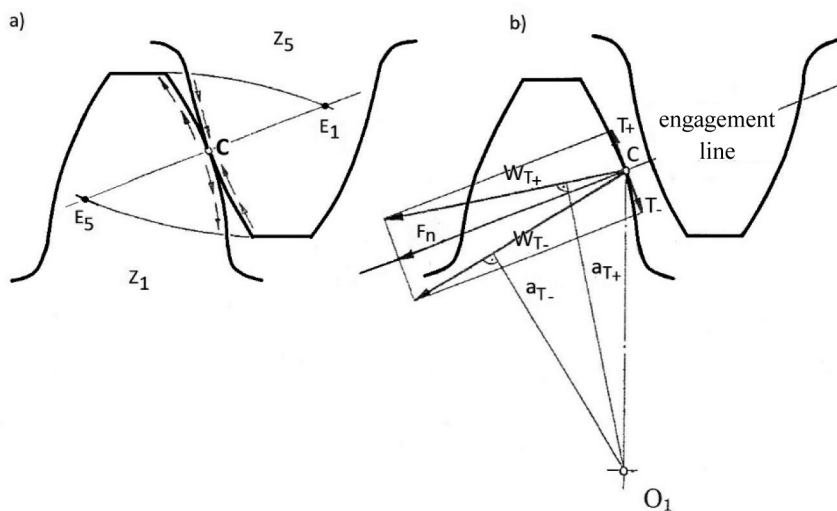


Fig. 4. Normal bilateral engagement: a) model of engagement of gear z_1 with gear z_5 , b) inter-tooth forces in pitch Point C
Rys. 4. Zazębianie dwustronne normalne: a) model zazębiania kola z_1 z kołem z_5 , b) siły międzyzębne w biegunie zazębiania C

Let the purpose of the considered gear pair be to transfer the torque M_1 as soon as the point of engagement of the cooperating involute teeth outlines has been located near the pitch point, and, at the same time, it is a part of the addendum of the driving gear z_1 . In this point of engagement, the normal force F_N appears and so does the friction force T_+ acting in the direction tangential to the teeth outline. The normal force F_N and the friction force T_+ can be replaced with the resultant force W_{T+} , whose purpose is to transfer the torque M_1 . By using the resultant force W_{T+} and its arm with a length a_{T+} , the following equation for the torque M_1 can be proposed:

$$M_1 = W_{T+} \times a_{T+} \quad (1)$$

A similar analysis can be carried out for the point of engagement of the cooperating teeth located near the pitch point and lying on the dedendum of the driving tooth. In this case, the normal force F_N and the friction force T_- which was replaced by the resultant force W_{T-} will have the action arms with a length a_{T-} . Therefore, an expression for the torque M_1 may be written in the following form:

$$M_1 = W_{T-} \times a_{T-} \quad (2)$$

The expressions (1) and (2) may be written after equating as follows:

$$M_1 = W_{T+} \times a_{T+} = W_{T-} \times a_{T-} \quad (3)$$

Based upon the Expression (3), one can determine a relationship between the resultant force W_{T+} linked to the addendum of the tooth and the resultant force W_{T-} linked to the dedendum of the tooth:

$$W_{T+} = W_{T-} \times (a_{T-} / a_{T+}) \quad (4)$$

Based on the Equation (4) and Fig. 4, it can be concluded that the quotient a_{T-} / a_{T+} will always be less than one, thus the value of the force W_{T-} acting at the dedendum will always be more than the value of the force W_{T+} acting at addendum with the same torque M_1 . The greater force value also generates higher contact stresses, and thus they accelerate the fatigue wear of the surface layer due to pitting.

Many experimental studies of the authors in the scope of contact fatigue strength of gears [L. 7–10] confirm that the first traces of pitting wear emerge on the dedendum of a gear. In the inter-tooth spaces of a gear pair, no matter whether the model experimental research or real-object research is dealt with, there is

oil as a lubricant [L. 11, 12]. Apart from its lubricating role, the oil has also a detrimental effect consisting in penetration into microcracking gaps, which, in turn, results in eroding the surface layer. In Fig. 5, there is shown a mechanism of this destructive phenomenon by using the example of the gear pair $z_1:z_5$ taken from the considered gear train (Fig. 1).

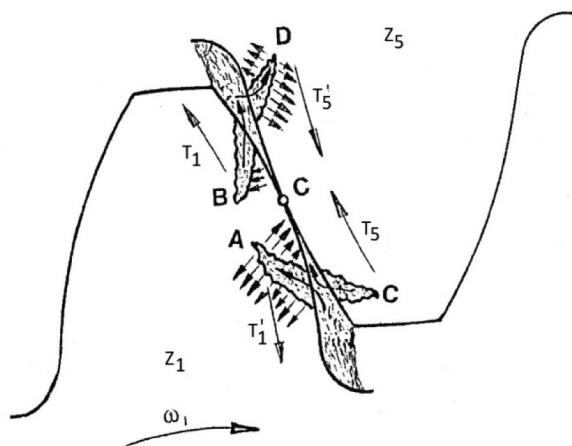


Fig. 5. Destruction of the top layer of gear pair in normal bilateral engagement

Rys. 5. Destrakcja warstwy wierzchniej pary zębatej zazębie-
nia dwustronnego normalnego

The gear pair in Fig. 5 is in the normal bilateral engagement, where the gear z_1 is a driving gear with an angular velocity ω_1 , and the gear z_5 is a driven gear, and this makes it possible to determine the senses of the friction forces T_1 and T_5 . Senses of the friction forces on the addendum and dedendum are different, so the cracking directions will also be different, because the cracks propagate into the depth of the top layer in the opposite direction to the friction forces.

By using Fig. 5, it is possible to do an analysis of destructive action of the oil penetrating into the microcracking gaps. Oil penetrating into Gap A during a contact of the cooperating gears z_1 and z_5 is encased by a tooth of the gear z_5 . Subsequently, the tooth of the gear z_5 presses on the portion of material above Gap A and makes it bend, thereby elevating the oil pressure in the crack. Periodic occurrence of such bending during the gear train operation leads to fatigue chipping in this portion of material. On a dedendum, there are usually more than one gaps described, but an erosion mechanism is the same as in the case of Gap A.

On the way of displacement of the cooperating teeth's contact point, Gap B may come up on the addendum of the driving gear. An erosive action of the oil in this gap is of a different character than in Gap A. Essential is a position where the lower edge of the gap comes into contact with the tooth of the gear z_5 and is bent before Gap B has been closed. This bent will reduce the gap volume and squeeze the oil out of it.

While considering Gap C on the addendum of a tooth of the driven gear z_5 , it is observed that the oil is squeezed out of it in the same way as from Gap B of the driving gear z_1 . Further displacement of the point of engagement of the cooperating teeth of the gears z_1 and z_5 reaches Gap D located on the dedendum of the driven gear tooth z_5 . The oil encased in Gap D will stimulate erosion in the top layer of the gear dedendum z_5 , like in Gap A on the dedendum of the gear z_1 .

UNILATERAL PRE-PITCH POINT ENGAGEMENT

Unilateral pre-pitch point engagement is characterized in that the total line of action is located on one side of the pitch Point C [L. 4, 6]. For the gear pair $z_1:z_5$ the origin of the line of action always lies at Point E_5 , whereas its end may be at Point C or before Point C, depending on the correction factor x_1 . The position of the line of action for the gear pair $z_1:z_5$ with the correction factors $x_1 = -1$ and $x_5 = +1$ is shown in Fig. 6.

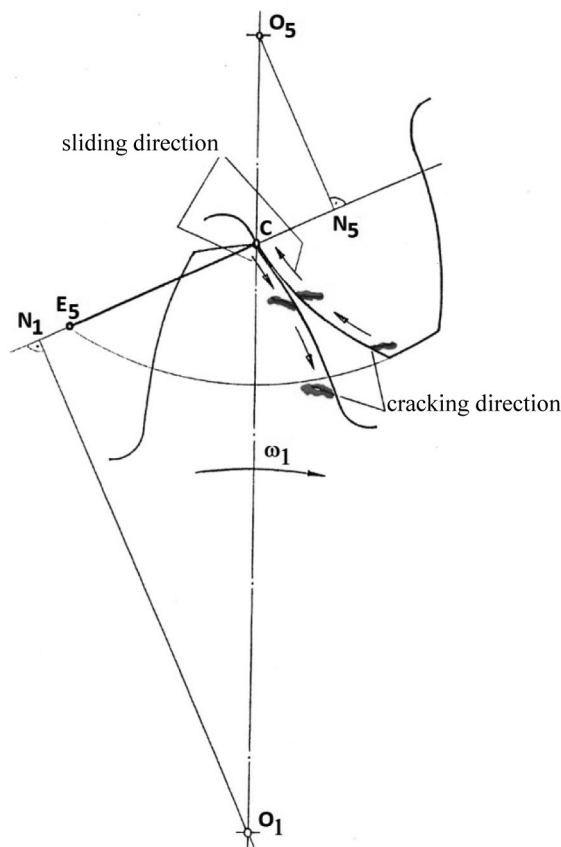


Fig. 6. Position of line of action in unilateral pre-pitch point engagement

Rys. 6. Położenie odcinka przyporu w zazębie-
niu jednostronnym przedbiegunowym

If the correction factor $x_1 < -1$, then the line of action ends before Point C. The correction factor

$x_1 = -1$ of the gear z_1 causes the total depth as if to comprise only a dedendum. Meanwhile, the total depth of the tooth of the gear z_5 with the correction factor $x_5 = +1$ is only an addendum. Accordingly, the kinematics of the engagement shown in Fig. 6 is characterized by the fact that the slip vector's sense (in contrast to the standard bilateral engagement) is still the same. Slippage direction and friction forces determine a cracking direction in the top layer on the effective surface of the gears z_1 and z_5 shown in Fig. 7.

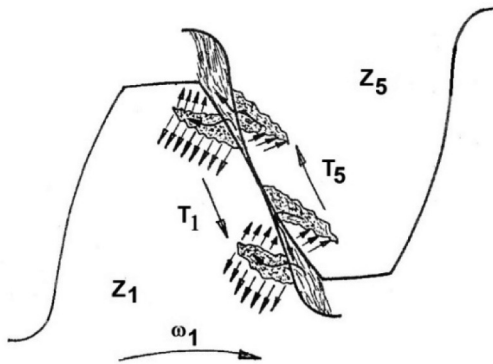


Fig. 7. Destruction of the top layer of the gear pair $z_1:z_5$ in the unilateral pre-pitch point engagement

Rys. 7. Destrakcja warstwy wierzchniej pary zębatej z_1/z_5 zążeńia jednostronnego przedbiegunowego

The oil penetrating into the gaps of the top layer of the driving gear z_1 acts expansively, and an erosive process takes place as depicted in Fig. 5. On the other

hand, a mechanism that proceeds in the gaps of a driven gear z_5 is the same as in Gap C of the normal bilateral engagement.

UNILATERAL POST-PITCH POINT ENGAGEMENT

Unilateral post-pitch point engagement is characterized in that the total line of action is located on one side of the pitch Point C [L. 4, 6]. The line of action is located on the side of a driven gear and is limited by the origin Point C and the end Point E_1 , as shown in Fig. 8.

The position of the action line in Fig. 8 relates to the gear pair $z_1:z_5$ with the correction factors $x_1 = +1$ and $x_5 = -1$, respectively. Comparing the engagement from Figs. 6 and 8, one can observe the opposite senses of the slip vector, opposite senses of the friction force, and opposite cracking directions on the working surfaces of the cooperating teeth. The friction force T_+ in the unilateral post-pitch point engagement is directed constantly towards the exterior of the gear, which creates an advantageous set-up for the tooth load by extending the arm a_{T+} , on which acts the resultant W_{T+} (this is proved by Equation 4).

The resultant W_{T+} in the unilateral post-pitch point engagement is less than the resultant W_T in the unilateral pre-pitch point engagement, so its destructive effect on the top layer within the working depth of the cooperating teeth is smaller. In this kind of engagement, there is also observed a destructive impact of the oil as a lubricant penetrating into microcracks in the top layer, which is shown in Fig. 9.

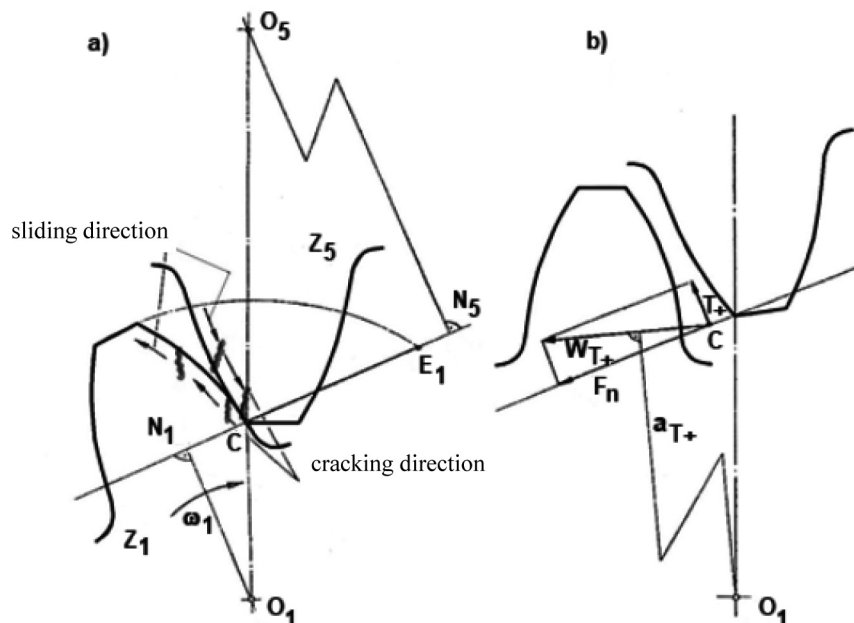


Fig. 8. Position of the line of action in unilateral post-pitch point engagement

Rys. 8. Położenie odcinka przyporu w zążeńiu jednostronnym pozabiegunowym

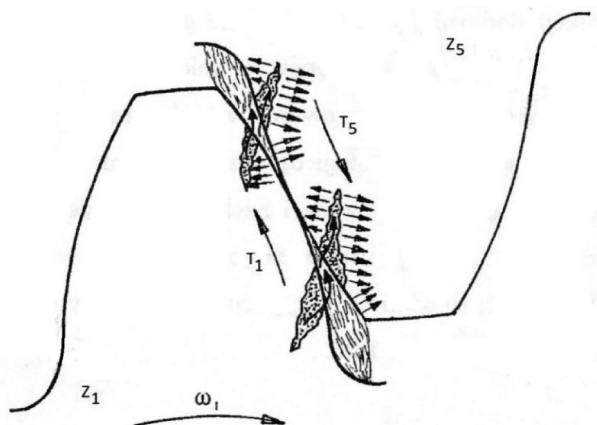


Fig. 9. Destruction of the top layer of the gear pair $z_1:z_5$ in the unilateral post-pitch point engagement

Rys. 9. Destrakcja warstwy wierzchniej pary zębatej $z_1:z_5$ za-
zębienia jednostronnego pozabiegunowego

Comparing **Figs. 7 and 9**, one can observe a sort of “anti-symmetry” in the similarity of the mechanism of the top layer destruction in the unilateral pre- and post-pitch point engagement. The similarity is that a tooth of a driving gear in the case of the unilateral pre-pitch point engagement is affected by the same destructive mechanism as a driven gear tooth in the unilateral post-pitch point engagement. A similar “anti-symmetry” can be applied with respect to the tooth of a driven gear in the unilateral pre-pitch point engagement and to the tooth of a driving gear in the unilateral post-pitch engagement.

It is necessary to remember, however, that the selection of a unilateral engagement, independently of whether it is to be a pre- or post-pitch point one, is limited to some extent by the number of teeth that the gears should have. It depends upon the quantity of the gear teeth and what value of a correction factor may be used. The commonly known criterion for using the positive correction is tooth easing. Meanwhile, the criterion for using a negative correction is undercutting the dedendum.

NUMERICAL TESTS OF CONTACT STRESSES AND INTER-TOOTH SLIDING

Numerical tests were carried out on a complete power shift transmission with six gear ratios, calculating contact stress and interdental slip at characteristic contact points, using a proprietary computer program [L. 7]. Characteristic concurrent contact on the active surface of the tooth profile reflecting the cooperation of the toothed pair z_1/z_5 , measured in diameters: d_{E1} – beginning of actual profile, d_{B1} – end of two-pair engagement zone, beginning of two-pair engagement zone, d_C – central point of engagement or pitch point, d_{B5} – end of one-pair engagement zone, a beginning of two-pair engagement zone, d_{E5} – end of actual tooth profile, end of two-pair engagement zone, are shown in **Fig. 10**.

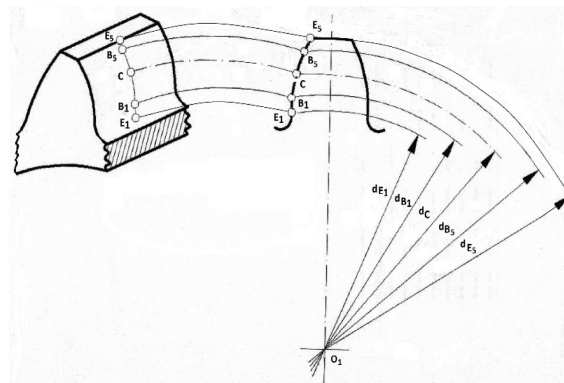


Fig. 10. Characteristic points of engagement gear pair $z_1:z_5$

Rys. 10. Charakterystyczne punkty przyporu pary zębatej $z_1:z_5$

The characteristic points visible in **Fig. 10** and their position on the engagement line with the measure of the radius of curvature of the involute (the active surface of the gear work together has the involute profile) are shown in **Fig. 11**.

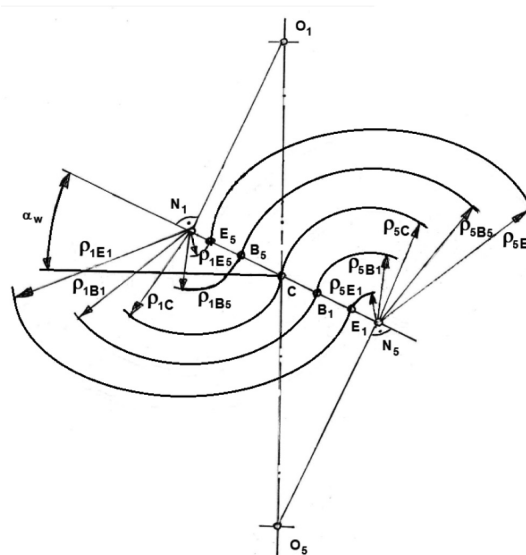


Fig. 11. Position of the characteristic points on the engagement line

Rys. 11. Położenie charakterystycznych punktów na linii przyporu

Contact stresses being a measure of the resistance of the surface layer to tribological wear were determined using a computer program [L. 10] for all gear pairs in the pre-, post-pitch, and normal engagement forming the investigated gearbox. Stress results are presented in **Table 1**.

At the same characteristic point of engagement (except Point C, where the slip speed is always zero), the slip value was calculated for each gear pair in the appropriate gear ratio. Gear pairs in a normal engagement achieve a slip speed (at an input speed of $n = 2000 \text{ min}^{-1}$) at characteristic contact points, as shown in **Table 2**.

Table 1. Contact stresses σ_H [MPa] in gear pairsTabela 1. Naprężenia kontaktowe σ_H [MPa] w parach zębatych

Gear pair	Type of gearing		
	pre-pitch	post-pitch	normal
z_1/z_5	1148 / 1049	1176 / 1176	1152 / 1112
z_6/z_9	1182 / 1067	1122 / 1134	1145 / 1122
z_{10}/z_{12}	1260 / 1067	1160 / 1160	1163 / 1090
z_3/z_7	1049 / 1116	1176 / 1122	1112 / 1095
z_8/z_{11}	1050 / 1050	1071 / 1199	1143 / 1183
z_2/z_4	1183 / 1078	1070 / 1170	1182 / 1182
z_3/z_5	1186 / 1049	1157 / 1176	1140 / 1112

Table 2. Slip values [m*s⁻¹] in normal gear engagementTabela 2. Wartości poślizgu [m*s⁻¹] w parach zębatych o zazębieniu normalnym

Gear ratio	Gear pair							Contact point
	z_1/z_5	z_6/z_9	z_{10}/z_{12}	z_3/z_7	z_8/z_{11}	z_2/z_4	z_3/z_5	
1	2.759	1.999	1.476					E ₁
	1.783	1.231	0.720					B ₁
	1.663	1.217	0.594					B ₃
	2.759	2.013	1.601					E ₅
2	2.759		2.526	2.695				E ₁
	1.783		1.232	1.556				B ₁
	1.663		1.018	1.663				B ₃
	2.759		2.741	2.617				E ₅
3	2.759			2.695	4.191			E ₁
	1.783			1.556	1.750			B ₁
	1.663			1.663	1.807			B ₃
	2.759			2.617	4.134			E ₅
4		1.999	1.476			4.029	2.759	E ₁
		1.231	0.720			1.465	1.783	B ₁
		1.217	0.594			1.465	2.880	B ₃
		2.013	1.601			4.029	2.880	E ₅
5			2.526	2.695		4.029	2.759	E ₁
			1.232	1.556		1.465	1.783	B ₁
			1.018	1.633		1.465	2.880	B ₃
			2.741	2.617		4.029	2.880	E ₅
6				2.695	4.191	4.029	2.759	E ₁
				1.556	1.750	1.465	1.783	B ₁
				1.633	1.807	1.465	2.880	B ₃
				2.617	4.134	4.029	2.880	E ₅

The slip speed in each case was calculated according to the following equations [L. 6]:

$$\begin{aligned}
 v_{SE_1} &= |\omega_1 * \rho_{1E_1} - \omega_5 * \rho_{5E_1}| \\
 v_{SB_1} &= |\omega_1 * \rho_{1B_1} - \omega_5 * \rho_{5B_1}| \\
 v_{SC} &= |\omega_1 * \rho_{1C} - \omega_5 * \rho_{5C}| - \\
 v_{SB_5} &= |\omega_1 * \rho_{1B_5} - \omega_5 * \rho_{5B_5}| \\
 v_{SE_5} &= |\omega_1 * \rho_{1E_5} - \omega_5 * \rho_{5E_5}|
 \end{aligned}
 \tag{5}$$

where

ω_1 – angular velocity of the gear z_1 ,

ω_5 – angular velocity of the gear z_5 ,

ρ_1 – radius of curvature of the outline of an involute gear of gear 1 at points respectively: E_1, B_1, C, B_5, E_5 ,

ρ_5 – radius of curvature of the involute gear outline of gear 5 respectively at points: E_1, B_1, C, B_5, E_5 .

The same gear pairs as in the normal bilateral gearing, but with a correction for a unilateral pre-pitch gearing (driving gear with correction factor -1, driven gear with correction factor +1) at the same input speed value of $n = 2000 \text{ min}^{-1}$ achieve the slip speeds shown in **Table 3**.

Table 3. Slip values [m^*s^{-1}] in pre-pitch gear engagement

Tabela 3. Wartości poślizgu [m^*s^{-1}] w parach zębatych o zazębieniu przedbiegunowym

Gear ratio	Gear pairs							Contact Point
	z_1/z_5	z_6/z_9	z_{10}/z_{12}	z_5/z_7	z_8/z_{11}	z_2/z_4	Z_3/z_5	
1	0.729	0.491	0.399					E_1
	5.271	3.721	1.797					B_1
	1.059	0.640	0.566					B_5
	5.602	3.870	2.761					E_5
2	0.729		0.682	5.241				E_1
	5.271		3.076	0.991				B_1
	1.059		0.968	4.637				B_5
	5.602		4.726	0.387				E_5
3	0.729			5.241	0.183			E_1
	5.271			0.991	5.757			B_1
	1.059			4.637	1.641			B_5
	5.602			0.387	7.582			E_5
4		0.491	0.399			0.730	0.090	E_1
		3.721	1.797			4.764	4.633	B_1
		0.640	0.566			1.514	1.059	B_5
		3.870	2.761			7.007	5.602	E_5
5			0.682	5.241		0.730	0.090	E_1
			3.076	0.991		4.764	4.633	B_1
			0.968	4.637		1.514	1.059	B_5
			4.726	0.387		7.007	5.602	E_5
6				5.241	0.183	0.730	0.090	E_1
				0.991	5.757	4.764	4.633	B_1
				4.637	1.641	1.514	1.059	B_5
				0.387	7.582	7.007	5.602	E_5

The application of the correction factor +1 for the driving gear and -1 for the driven gear results in a unilateral post-pitch gearing. For such a gearing, the slip values for all gear pairs at the characteristic points of engagement are shown in **Table 4**.

In **Tables 2 to 4**, blank positions mean that a given gear pair is not involved in the transmission of the rotational movement at a given gear ratio, even though all gears remain in the gear engagement.

Table 4. Slip values [$m*s^{-1}$] in post-pitch gear engagementTabela 4. Wartości poślizgu [$m*s^{-1}$] w parach zębatych o zazębieniu pozabiegunowym

Gear ratio	Gear pair							Contact point
	z_1/z_5	z_6/z_9	z_{10}/z_{12}	z_5/z_7	z_8/z_{11}	z_2/z_4	Z_3/z_5	
1	5.645	4.153	2.966					E_1
	1.103	0.923	0.771					B_1
	4.319	3.158	1.960					B_5
	0.223	0.073	0.236					E_5
2	5.645		5.077	0.209				E_1
	1.103		1.319	4.041				B_1
	4.319		3.354	1.083				B_5
	0.223		0.404	5.333				E_5
3	5.645			0.209	8.052			E_1
	1.103			4.041	2.112			B_1
	4.319			1.083	5.331			B_5
	0.223			5.333	0.609			E_5
4		4.153	2.966			8.006	5.649	E_1
		0.923	0.771			2.513	1.107	B_1
		3.158	1.960			4.837	4.319	B_5
		0.073	0.236			0.656	0.223	E_5
5			5.077	0.209		8.006	5.649	E_1
			1.319	4.041		2.513	1.107	B_1
			3.354	1.083		4.837	4.319	B_5
			0.404	5.333		0.656	0.223	E_5
6				0.209	8.052	8.006	5.649	E_1
				4.041	2.112	2.513	1.107	B_1
				1.083	5.331	4.837	4.319	B_5
				5.333	0.609	0.656	0.223	E_5

DISCUSSION OF NUMERICAL SURVEY RESULTS

During analysing the values of contact stresses in **Table 1**, it is noted that the gear z_5 , which is working together with the gears z_1 , z_3 , and z_7 , has the lowest value of $\sigma_H = 1049$ MPa in the pre-pitch gearing. On the other hand, the z_8/z_{11} gear pair in the pre-pitch engagement is subjected to contact stress $\sigma_H = 1050$ MPa, both for z_8 and z_{11} gears. In the case of out pitch engagement, the lowest values of contact stresses, $\sigma_H = 1070$ MPa, are found in the gear z_2 which work together with the gear z_4 . In a bilateral normal engagement in a gear z_{12} gear pair z_{10}/z_{12} , the lowest contact stress, $\sigma_H = 1090$ MPa, is greater than the lowest stress occurring in a pre-pitch or post-pitch engagement. Out of all 12 gears present in the investigated gearbox, the highest number of load cycles within the specified service life will be performed by the gear z_5 , because it works together with the gear pairs: z_1/z_5 , z_3/z_5 , and z_5/z_7 . Therefore, the lowest value

of contact stress, $\sigma_H = 1049$ MPa, in the unilateral pre-pitch engagement is important for this gear. The values of the inter-tooth slip shown in **Tables 2, 3**, and **4** for gear pair z_1/z_5 for the respective gearing (normal bilateral engagement, pre-pitch unilateral engagement, post-pitch unilateral engagement) are the same at each gear ratio level (1 to 3) at the respective points of engagement. This is due to the constant speed of $n = 1800$ rpm of Shaft I input, on which the driving gear z_1 is placed, forming a gear pair with the gear z_5 . Moreover, on Shaft I input, there is a z_2 driving gear work together with a gear z_4 , which realizes gear ratios from 4 to 6. In next pairs of teeth, the numerical values of the slip already result from the respective gear ratios. It is noted in **Tables 2, 3**, and **4** that the numerical values of slip in the respective toothed pairs and at the corresponding points of engagement in gear ratio 1 to 3 correspond to the numerical values of slip of these pairs involved in gear ratio 4 to 6. This is shown in **Figs. 2** and **3**, where the number of teeth in the gear z_2 equals the number of teeth in the gear z_4 . The

highest slip value in both bilateral normal and unilateral pre-pitch and post-pitch engagement is found in the z_8/z_{11} and z_2/z_4 gear pairs at the extreme point of engagement E_1 and E_2 , where the top of the driving gear tooth is in contact with the beginning of the active outline of the driven gear. On the active surfaces of the gear z_5 in three gears pairs (z_1/z_5 , z_5/z_7 , z_3/z_5), an inter-tooth slide with the lowest value of $V_s = 0.09 \text{ m*s}^{-1}$ at the E_1 pre-pitch point of engagement (**Table 3**) of the gear pair z_3/z_5 to the highest value of $V_s = 5.649 \text{ m*s}^{-1}$ of the same gear in the post-pitch engagement (**Table 4**) at the E_1 out-pitch point of engagement. The minimum and maximum inter-teeth slip range for normal bilateral engagement are much smaller, and for z_3/z_5 gear pair are in the range of 1.783 to 2.88 m*s^{-1} (**Table 2**).

SUMMARY

Conducting numerical research with multi-criteria optimization enables the implementation of multi-variant design solutions and then selecting the best solution based on the adopted criteria. The complete

gearbox shows that the gear z_5 in combination with the z_1 , z_3 , and z_7 gears is subjected to the lowest contact stresses in the case of unilateral pre-pitch engagement. This is a beneficial engagement case for the z_5 gear due to its number of load cycles in service, which is the largest of all in twelve gears. Unilateral pre-pitch engagement is obtained by applying a correction factor $x = -1$ for the driving gear and $x = +1$ for the driven gear. The correction factor $x = +1$ in the driving gear and $x = -1$ in the driven gear provides a unilateral out of pitch engagement.

The use of unilateral engagement is also beneficial because the sense of the slip vector on the active surfaces of the work together tooth sides is always the same. No change in the sense of a slip vector also ensures a constant sense of friction forces, which, in the case of a bilateral normal engagement, change when passing through the central point of the engagement (the gearing pole). The constant sense of a slip vector and friction forces has a positive effect on the lubrication quality and stability of the gearbox work, which together reduces the vibroacoustic activity of the entire system associated with the gearbox.

REFERENCES

1. Li Baogang, Sun Dongye, Hu Minghui, ZhouXingyu, Liu Junlog, Wang Dongyang: Coordinated control of gear shifting proces with multiple clutches for power shift transmission. *Mechanism and Machine Theory*, vol. 140, October 2019, pp. 274–291.
2. Molari G., Sedoni E.: Experimental evaluation of power losses in a power shift agricultural tractor transmission. *Biosystems Engineering*, vol. 100, issue 2, June 2008, pp. 177–183.
3. Mara Tanelli, Giulio Panzani, Sergio M. Savaresi, Carlo Pirola: Transmission control for power shift agricultural tractors: Design and end – of – line automatic tuning. *Mechatronics*, vol. 21, issue 1, February 2011, pp. 285–297.
4. Rohonyi W.: Untersuchung verschiedener Profilverschiebungssysteme aufgrund elasto-hydrodynamischer Erkenntnisse. *Konstruktion* 26, nr 3, 1974.
5. Baogang Li, Dongye Sun, Munghui Hu, Junlog Liu: Automatic starting control of tractor with a novel power shift transmission. *Mechanism and Machine Theory*, vol. 131, January 2019, pp. 75–91.
6. Muller L.: Przekładnie zębate projektowanie. WNT, Warszawa 1996.
7. Martyna M., Zwolak J.: Software with multi-criteria optimization PRZEKŁADNIA. www.gearbox.com.pl.
8. Zwolak J., Martyna M.: The analysis of the slippage and contact stress in the meshing of the power shift type gear. *Tribologia*, nr 5, 2016, pp. 229–241.
9. Zwolak J., Palczak A.: The effect of the gear teeth finishing method on the properties of the teeth surface layer and its resistance to the pitting wear creation. *Journal of Central South University*, January 2016, vol. 23, issue 1, pp. 68–76.
10. Zwolak J., Martyna M.: Analysis of contact and bending stresses in gearbox switching under load. *Tribologia*, nr 4, 2017, pp. 133–138.
11. Amarnath M., Sujatha C., Swarnamani S.: Experimental studies on the effects of reduction in gear tooth stiffness and lubricant film thickness in a spur geared system. *Tribology International*, vol. 42, issue 2, February 2009, pp. 340–352.
12. Yiyao Jiang, Xiaozhou Hu, Shunjun Hong, Pingping Li, Minggui Wu: Influences of an oil guide device on splash lubrication performance in a spiral bevel gearbox. *Tribology International*, vol. 136, August 2019, pp. 155–164.